J|A|C|S
ARTICLES
Published on Web 12/24/2002

Energetic and Stereochemical Effects of the Protein Environment on Substrate: A Theoretical Study of Methylmalonyl-CoA Mutase

Markus J. Loferer,[†] Ben M. Webb,[‡] Guy H. Grant,[‡] and Klaus R. Liedl*,[†]

Contribution from the Institute of General, Inorganic, and Theoretical Chemistry, University of Innsbruck, Innrain 52a, A-6020 Innsbruck, Austria, and Physical and Theoretical Chemistry Lab, University of Oxford, Central Chemistry Lab, South Parks Road, Oxford, OX1 3QH, United Kingdom

Received October 11, 2002; E-mail: klaus.liedl@uibk.ac.at

Abstract: QM/MM methods were used to study the isomerization step from (2*R*)-methylmalonyl-CoA to succinyl-CoA. A pathway via a "fragmentation−recombination" mechanism is ruled out on energetic grounds. For the other radicalic pathway, involving an addition recombination step, geometries and vibrational contributions have been determined, and a barrier height of 11.70 kcal/mol was found. The effect of adjacent hydrogen-donating groups was found to reduce the energy barrier by 1−2 kcal/mol each and thus to provide a significant catalytic effect for this reaction. By means of molecular dynamics studies, the stereochemistry of the methylmalonyl-CoA mutase catalyzed reaction was examined. It is shown that TYR89 is essential for maintaining stereoselectivity of the abstraction of a hydrogen in the backreaction. The subsequent selective formation of one isomer of methylmalonyl-CoA is probably due to the presence of a bulky side chain.

Introduction

Methylmalonyl-CoA mutase catalyzes the isomerization of (2*R*)-methylmalonyl-CoA (*MMCoA*) to succinyl-CoA (*Succ-CoA*). Together with glutamate mutase, this enzyme belongs to a class of B_{12} binding proteins which utilize adenosylcobalamin to create a radical[1−3] and thus facilitate a 1,2-migration of a fragment of the substrate. Other adenosylcobalamin-dependent isomerases facilitate the interchange of a hydroxy- or amino-group[4,5] or the reduction of nucleoside 5′-triphosphate to 2′-deoxynucleoside 5′-triphosphate.[6,7] All of these reactions are initiated by homolytic cleavage of the Co−C bond of adenosylcobalamin, and it is generally accepted that these are accelerated by a factor on the order of $10^{11}-10^{12}$ by the enzyme.[8,9] The exact mechanism is still poorly understood (an overview of the catalytic cycle is given in Figure 1); however, several factors might contribute to this high speed-up: the replacement of the lower axial base of the B_{12} cofactor by a protein-supplied histidine,[10−13] a deformation of the corrin ring,[14] and steric strain induced by substrate binding[15] might accomplish the destabilization of the Co−C bond. Although X-ray structures of the cleaved and uncleaved cofactor exist,[15−17] and computational studies have provided valuable support,[18−20] a clear picture has yet to emerge. For *MMCoA* mutase, in a consecutive step after cleavage of the Co−C bond, the radical located at the adenosyl moiety must be transferred to the substrate where a hydrogen is abstracted.[21] There is evidence for a large pre-steady-state kinetic isotope effect of 35 at 293 K,[22,23] which is indicative of quantum mechanical tunneling of a hydrogen atom. Kinetic coupling of homolysis and radical transfer[24] is also generally accepted. Because of the large distance between Co and substrate, concerted action is not probable, although there

[†] University of Innsbruck.
[‡] University of Oxford.

(1) Banerjee, R. *Biochemistry* **2001**, *40*, 6191−6198.
(2) Marsh, E. N. G.; Drennan, C. L. *Curr. Opin. Chem. Biol*. **2001**, *5*, 499−505.
(3) Frey, P. A.; Reed, G. H. *Arch. Biochem. Biophys*. **2000**, *382*, 6−14.
(4) Shibata, N.; Masuda, J.; Tobimatsu, T.; Toraya, T.; Suto, K.; Morimoto, Y.; Yasuoka, N. *Structure* **1999**, *7*, 997−1008.
(5) Toraya, T. *Cell. Mol. Life Sci*. **2000**, *57*, 106−127.
(6) Lawrence, C. C.; Gerfen, G. J.; Samano, V.; Nitsche, R.; Robbins, M. J.; Retey, J.; Stubbe, J. *J. Biol. Chem*. **1999**, *274*, 7039−7042.
(7) Licht, S. S.; Booker, S.; Stubbe, J. *Biochemistry* **1999**, *38*, 1221−1233.
(8) Banerjee, R. *Chem. Biol*. **1997**, *4*, 175−186.
(9) Chowdhury, S.; Banerjee, R. *Biochemistry* **2000**, *39*, 7998−8006.
(10) Padmakumar, R.; Taoka, S.; Padmakumar, R.; Banerjee, R. *J. Am. Chem. Soc.* **1995**, *117*, 7033−7034.
(11) Garr, C. D.; Sirovatka, J. M.; Finke, R. G. *Inorg. Chem*. **1996**, *35*, 5912−5922.
(12) Garr, C. D.; Sirovatka, J. M.; Finke, R. G. *J. Am. Chem. Soc.* **1996**, *118*, 11142−11154.
(13) Dong, S.; Padmakumar, R.; Banerjee, R.; Spiro, T. G. *J. Am. Chem. Soc.* **1999**, *121*, 7063−7070.
(14) Kraeutler, B.; Konrat, R.; Stupperich, E.; Faerber, G.; Gruber, K.; Kratky, C. *Inorg. Chem*. **1994**, *33*, 4128−4139.
(15) Mancia, F.; Evans, P. R. *Structure* **1998**, *6*, 711−720.
(16) Mancia, F.; Keep, N. H.; Nakagawa, A.; Leadley, P. F.; McSweeney, S.; Rasmussen, B.; BOsecke, P.; Diat, O.; Evans, P. R. *Structure* **1996**, *4*, 339−350.
(17) Mancia, F.; Smith, G. A.; Evans, P. R. *Biochemistry* **1999**, *38*, 7999−8005.
(18) Kozlowski, P. M. *Curr. Opin. Chem. Biol*. **2001**, *5*, 736−743.
(19) Dölker, N.; Maseras, F.; Lledos, A. *J. Phys. Chem. B* **2001**, *105*, 7564−7571.
(20) Jensen, K. P.; Sauer, S. P. A.; Liljefors, T.; Norrby, P.-O. *Organometallics* **2001**, *20*, 550−556.
(21) Gruber, K.; Reitzer, R.; Kratky, C. *Angew. Chem., Int. Ed*. **2001**, *40*, 3377−3380.
(22) Chowdhury, S.; Banerjee, R. *J. Am. Chem. Soc*. **2000**, *122*, 5417−5418.
(23) Dybala-Defratyka, A.; Paneth, P. *J. Inorg. Biochem*. **2001**, *86*, 681−689.
(24) Padmakumar, R.; Padmakumar, R.; Banerjee, R. *Biochemistry* **1997**, *36*, 3713−3718.

10.1021/ja028906n CCC: $25.00 **© 2003 American Chemical Society**

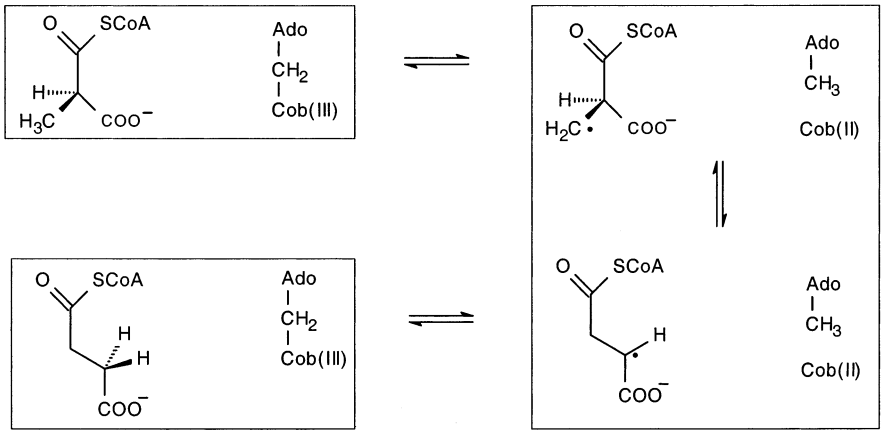

Figure 1. Proposed mechanism for the rearrangement of *MMCoA* to *SuccCoA* catalyzed by *MMCoA* mutase. In the top row, the Co−C bond is broken, and the B_{12} cofactor abstracts a hydrogen atom from the substrate. The next step in the catalytic cycle (right box) is the rearrangement of the substrate, which is a topic of this publication. In the bottom row, the product (*SuccCoA*) recombines with a hydrogen atom from adenosine to re-form the initial cofactor.

is no evidence for the existence of the adenosyl radical as a discrete intermediate species, which requires in particular that the ongoing steps kinetically control Co−C homolysis and thus prohibit an accumulation of radicals. The consecutive step is the isomerization of the substrate radical,[25] which is what the first part of this study focuses on. In the ongoing step, a hydrogen atom is reabstracted by deoxyadenosine, and recombination of deoxyadenosine and cobalamine and product release complete the catalytic cycle.

Several pathways have been proposed for the mechanism of the 1,2-rearrangement of (2*R*)-*MMCoA* to *SuccCoA*,[26,27] including carbanionic and organo-cobalt species. However, the formation of a cobalt-bound substrate complex seems very unlikely from the arrangement found in crystal structures,[16] and from numerous experiments with model reactions[28−32] or in enzyme,[33−35] a mechanism involving radicals seems natural.

This rearrangement can be accomplished by an intramolecular addition−elimination mechanism. Such a pathway requires the existence of a cyclopropyloxy-species as a short-lived intermediate or transition state complex and involves migration of the thioester group of the substrate. An intramolecular radical addition to the carbonyl carbon gives a transient cyclopropyloxy radical which undergoes then a ring-opening elimination reaction to form the product[32] (Figure 2a).

As a second viable option, a fragmentation−recombination mechanism, as is also assumed for glutamate mutase,[36−39] is

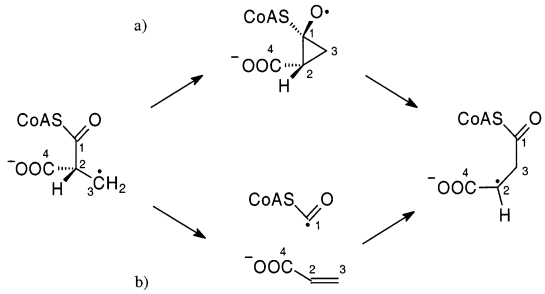

Figure 2. Possible pathways for the rearrangement of the *MMCoA* radical. Pathway a: Addition−elimination mechanism. An intramolecular radical addition to the carbonyl carbon is followed by a ring-opening elimination. Pathway b: Fragmentation−recombination mechanism. The formation of a formyl radical and acrylate is followed by a radical addition to form the product.

proposed and involves a homolytic bond fission (Figure 2b) to give a formyl radical and ethylene. By an intermolecular radical addition, the product is then formed.

Apart from the catalytically advantageous effects from a polar electrostatic environment and/or enzymatic complementarity to a substrate bound as a transition state analogue, explicit site-directed catalysis by partial proton transfer to the acyl oxygen of the migrating group might contribute to lowering of the activation energy.[40−42] A similar effect has also been discussed in the context of the B_{12}-dependent diol dehydratase,[43,44] and a part of this study is designated to focus on this phenomenon.

Another peculiarity of *MMCoA* mutase is the "imperfect" stereochemistry of the rearrangement back-reaction of *SuccCoA* to (2*R*)-*MMCoA*. Isotope labeling experiments[45,46] show that during the hydrogen abstraction step, stereoselectivity is not perfect, as one of the two enantiotopic hydrogens is frequently but not exclusively abstracted from succinyl CoA. However,

(25) Hull, W. E.; Michenfelder, M.; Retey, J. *Eur. J. Biochem.* **1988**, *173*, 191−201.
(26) Halpern, J. *Science* **1985**, *227*, 869−875.
(27) He, M.; Dowd, P. *J. Am. Chem. Soc.* **1998**, *120*, 1133−1137.
(28) Bidlingmaier, G.; Flohr, H.; Kempe, U. M.; Krebs, T.; Retey, J. *Angew. Chem., Int. Ed. Engl.* **1975**, *14*, 822−823.
(29) Scott, A. I.; Hansen, J. B.; Chung, S.-K. *J. Chem. Soc., Chem. Commun.* **1980**, 388−389.
(30) Wollowitz, S.; Halpern, J. *J. Am. Chem. Soc.* **1984**, *106*, 8319−8321.
(31) Dowd, P.; Wilk, B.; Wilk, B. K. *J. Am. Chem. Soc.* **1992**, *114*, 7949−7951.
(32) He, M.; Dowd, P. *J. Am. Chem. Soc.* **1996**, *118*, 711.
(33) Zhao, Y.; Such, P.; Retey, J. *Angew. Chem., Int. Ed. Engl.* **1992**, *31*, 215−216.
(34) Zhao, Y.; Abend, A.; Kunz, M.; Such, P.; Retey, J. *Eur. J. Biochem.* **1994**, *225*, 891−896.
(35) Beatrix, B.; Zelder, O.; Kroll, F. K.; Örlygsson, G.; Golding, B. T.; Buckel, W. *Angew. Chem., Int. Ed. Engl.* **1995**, *34*, 2398−2401.
(36) Chih, H.-W.; Marsh, E. N. G. *Biochemistry* **1999**, *38*, 13684−13691.
(37) Chih, H.-W.; Marsh, E. N. G. *J. Am. Chem. Soc.* **2000**, *122*, 10732−10733.
(38) Reitzer, R.; Gruber, K.; Jogl, G.; Wagner, U. G.; Bothe, H.; Buckel, W.; Kratky, C. *Structure* **1999**, *7*, 891−902.
(39) Wetmore, S. D.; Smith, D. M.; Golding, B. T.; Radom, L. *J. Am. Chem. Soc.* **2001**, *123*, 7963−7972.
(40) Merkelbach, I. I.; Becht, H. G. M.; Buck, H. M. *J. Am. Chem. Soc.* **1985**, *107*, 4037−4042.
(41) Smith, D. M.; Golding, B. T.; Radom, L. *J. Am. Chem. Soc.* **1999**, *121*, 1383−1384.
(42) Wetmore, S. D.; Smith, D. M.; Radom, L. *CHEMBIOCHEM* **2001**, *12*, 919−922.
(43) George, P.; Glusker, J. P.; Bock, C. W. *J. Am. Chem. Soc.* **1997**, *119*, 7065−7074.
(44) Smith, D. M.; Golding, B. T.; Radom, L. *J. Am. Chem. Soc.* **2001**, *123*, 1664−1675.
(45) Wöle, K.; Michenfelder, M.; König, A.; Hull, W. E.; Retey, J. *Eur. J. Biochem.* **1986**, *156*, 545−554.
(46) Michenfelder, M.; Hull, W. E.; Retey, J. *Eur. J. Biochem.* **1987**, *168*, 659−667.

the ongoing step is strictly selective for one of the isomers, and from the X-ray structure of *MMCoA* mutase complexed with substrate/inhibitors, it might be concluded that the position of Tyr89 is critical in controlling stereochemical selectivity[17] as it is conceivable that (2*S*)-*MMCoA* would collide with this residue upon formation.

In this work, we present QM/MM calculations as well as molecular dynamics simulations concerning the bound substrate. Two possible radicalic pathways for isomerization were examined in detail, and structures and energies for minimum energy geometries and the saddle point are presented. The influence of hydrogen bonding partners on the energetics of the system was examined by calculating the energy of several variants of the original system. Additionally, MD simulations were performed to elucidate further the interaction of the substrate with potential hydrogen bond donors but also to investigate the cryptic stereochemistry of *MMCoA* mutase. For this reason, three simulations of 1000 ps have been performed, where the wild-yype TYR89 and the "in silico" mutants TYR89PHE and TYR89GLY were the subject of interest.

Computational details are summarized in the second section; the third section presents results and discussion divided into two subsections dealing with QM/MM and MD studies. The conclusions are presented in the final section.

Computational Methods

With the availability of density functional methods in hybrid QM/MM potentials,[47] it is now possible to simulate enzymatic reactions in their natural environment to a good degree of quantitative accuracy at an affordable cost. Throughout this work, the energetics of all considered systems were studied by means of QM/MM methods.[48] All QM/MM calculations have been performed employing DFT methods with the B3LYP functional and a 6-31G(d) or a higher basis set for the QM part. The MM part and the coupling terms of the QM/MM Hamiltonian have been used as described in Lyne et al.[47] For single-point energies, enlarged basis sets (6-311+G(d,p)) were used.[1]A comparison with a 6-311++G(3d,f,2p) basis set for one of the systems showed relative energy differences of less than 0.4 kcal/mol. Thus, the smaller basis was considered to be sufficient for providing accurate energies. For the QM method of all QM/MM minimizations, an unrestricted approach (UDFT) was employed as it is implemented in GAMESS-US,[49] which was interfaced with CHARMM[50] version c28b2, and showed a low spin contamination (0.75−0.85 for doublet states).

QM-MM boundaries were handled with link atoms that cut across single bonds. Each link atom was treated as a proper QM atom and thus was exposed to the field of all surrounding point charges. Following other QM/MM-studies, the link atom was forced by bond and angle restraints to maintain its geometry.[51] The charge of the bordering MM atom was set to zero and redistributed to other atoms of the adjacent group to maintain electroneutrality. The basic QM system was the methylmalonic part of *MMCOA*, including the sulfur atom which was capped with a link atom. Extended QM regions comprised the imidazolic part of HIS244, the formamide part of GLN197, and the phenole part of TYR89, each terminated correspondingly with a link atom. The QM regions are depicted in Figure 3.

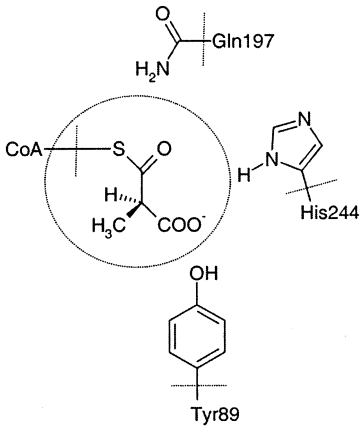

Figure 3. The subsystems which are computed by quantum mechanical methods are drawn. Oval box: The small quantum mechanics zone containing the reactive part of the substrate. Additional catalytically active residues which were included in the QM region are shown outside of the oval box. The dashed lines mark the QM/MM boundaries.

For the minimizations, the atoms of the QM region and all MM atoms in a 15 Å sphere around the geometrical center of the QM region, adding up to 1640 atoms, were allowed to move; the atoms outside this region were kept fixed for all geometries after an initial minimization. The TRAVEL module, as implemented in CHARMM,[52] was employed for stringent saddle point optimization. For this, a starting guess of a chain of points lying on the reaction path is required. By a series of energy maximizations along a reactive mode and minimizations in all space directions conjugate to that, a saddle point is iteratively constructed ("conjugate peak refinement"). Because of the large number of energy and gradient evaluations necessary, the movable atoms had to be restricted to a zone containing the QM atoms comprising 36 degrees of freedom. The exterior of this zone was then minimized with the atoms refined before being restrained to their position. This strategy is an extension of the approach by Zhang et al.,[53] with the inherent assumption that the reactive modes leading to a saddle point are closely localized around the center of reaction, which is also supported by a study of Cui et al.[54] At any rate, this strategy is preferable to adiabatic mapping, as no trivial reaction coordinate can be found here. All stationary points were verified by the calculation of numerical second derivatives and then corrected by the corresponding zero-point energies. The importance of the inclusion of quantum mechanical vibrational energies has recently been pointed out by Garcia-Viloca et al.[55] For this calculation, it was again necessary to restrict the number of degrees of freedom only to the essential ones. All link atoms were excluded from the evaluation and kept fixed. A steepest descent calculation, also implemented in the TRAVEL module, additionally verified the found transition state by connecting it with educt and product.

The 2.2 Å resolution X-ray structure of *MMCoA* mutase was used as the starting structure, together with *MMCoA* as substrate[17] (PDB ID: 4REQ), and was retrieved from the Protein Data Bank.[56] Charges for this molecule and the two dissociated adenosylcobalamin fragments were determined via an ESP method according to the Merz−Singh−Kollman scheme[57] as it is implemented in Gaussian 98.[58] Parameters for the corrinoid system were initially taken from the HEME parameters in CHARMM and were adapted and refined to reproduce the experi-

(47) Lyne, P. D.; Hodoscek, M.; Karplus, M. *J. Phys. Chem. A* **1999**, *103*, 3462−3471.
(48) Field, M. J.; Bash, P. A.; Karplus, M. *J. Comput. Chem*. **1989**, *6*, 700−733.
(49) Schmidt, M. W.; Baldridge, K. K.; Boatz, J. A.; Elbert, S. T.; Gordon, M. S.; Jensen, J. H.; Koseki, S.; Matsunaga, N.; Nguyen, K. A.; Su, S. J.; Windus, T. L.; Dupuis, M.; Montgomery, J. A. *J. Comput. Chem*. **1993**, *14*, 1347−1363.
(50) Brooks, B. R.; Bruccoleri, R. E.; Olafson, B. D.; States, D. J.; Swaminathan, S.; Karplus, M. *J. Comput. Chem*. **1983**, *4*, 187−217.
(51) Reuter, N.; Dejaegere, A.; Maigret, B.; Karplus, M. *J. Phys. Chem. A* **2000**, *104*, 1720−1735.
(52) Fischer, S.; Karplus, M. *Chem. Phys. Lett*. **1992**, *194*, 252−261.
(53) Zhang, Y.; Liu, H.; Yang, W. *J. Chem. Phys*. **2000**, *112*, 3483−3492.
(54) Cui, Q.; Karplus, M. *J. Am. Chem. Soc*. **2002**, *124*, 3093−3124.
(55) Garcia-Viloca, M.; Alhambra, C.; Truhlar, D. G.; Gao, J. *J. Chem. Phys*. **2001**, *114*, 9953−9958.
(56) Berman, H. M.; Westbrook, J.; Feng, Z.; Gilliland, G.; Bhat, T. N.; Weissig, H.; Shindyalov, I. N.; Bourne, P. E. *Nucleic Acids Res*. **2000**, *28*, 235−242.
(57) Singh, U. C.; Kollman, P. A. *J. Comput. Chem*. **1984**, *5*, 129−145.

mentally known geometries from classical MM minimizations in vacuo and in aqueous solution. For all other residues, standard parameters were used.[59] The enzyme was solvated with 473 TIP3P water molecules in a sphere with radius 25 Å around the reactive center, and a stochastic boundary treatment was used. The added water molecules were equilibrated by a series of minimizations and high-temperature MD runs until all cavities were filled and no more water molecules could be added.

MD Setup. For all simulations, a stochastic boundary setup was used.[60] All atoms confined in a sphere of 18 Å radius were treated by conventional molecular dynamics (reaction zone), whereas the atoms outside this sphere up to a shell with a radius of 25 Å were treated by stochastic dynamics,[61−63] and the atoms outside of that were kept fixed. A time step of 1 fs together with the SHAKE algorithm was employed. Conventional friction constants were employed, and the system was heated to room temperature over a period of 40 ps.

Results and Discussion

Energetics of Different Pathways. The settings mentioned in the Computational Methods section for the MD setup were mostly retained for the QM/MM minimizations. Differing from that, all atoms outside of a radius of 15 Å from the reactive center were kept fixed. The two pathways depicted in Figure 2 have been examined in detail. The numbering scheme is also given in Figure 2.

First, mechanism b in Figure 2 was examined. Adiabatic mapping along the bond C1−C2, which would dissociate in the course of the reaction, was performed. The energies as a function of the distance are shown in Figure 4. Following relaxation of the constraints, a stable intermediate, although at an energy of +27.48 kcal/mol as compared to that of the educt, was found, but only when the constrained distance C1−C2 exceeded 2.5 Å. The acrylic acid fragment then points toward the bound B_{12} cofactor and is thus probably destabilized by short-range nonbonded interactions (Figure 5A). To account for the correct stereochemistry, an additional rotation along the C2−C4 axis would be necessary. Because of the highly unstable intermediate found, this reaction path seems very unlikely and was, therefore, not pursued further.

For the mechanism involving a cyclopropyloxy-saddlepoint, a first guess was created by a structure obtained from an ab initio calculation in vacuo. For the saddle point optimization by the conjugate peak refinement method, this structure and those of the educt and product were used as input. The QM atoms were allowed to move, whereas all other atoms were kept fixed during the TRAVEL optimization. After this, the fixed atoms were minimized with the atoms previously optimized constrained to their new positions. After another iteration, the geometries remained unchanged. The geometries of all structures are shown in Figure 5B and C. A calculation of numerical frequencies showed all positive frequencies only for educt and product; for the saddle point, one imaginary frequency of $\nu = 307\ \mathrm{cm}^{-1}$ resulted in a zero-point correction energy of −0.21 kcal/mol. The validity of the found saddle point was additionally confirmed by calculation of a steepest-descent path, which connects the three found stationary points. This calculation was also performed with the TRAVEL module of CHARMM.

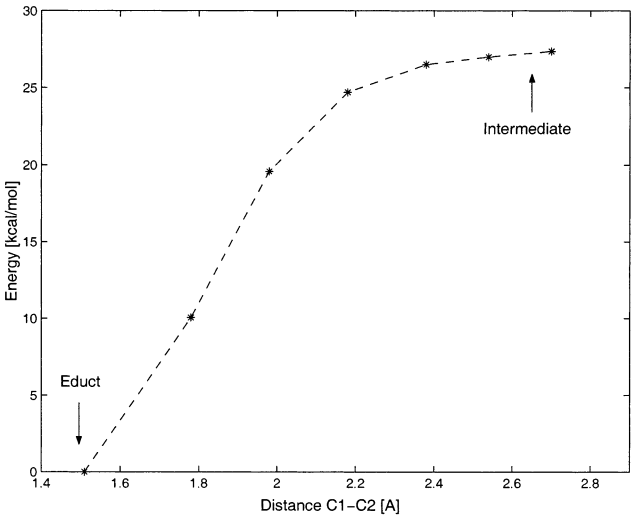

Figure 4. Energies along the reaction coordinate of the fragmentation−recombination pathway. The intermediate which was found when the distance constraint was relaxed is located at a distance of 2.68 Å. The calculated energy points are highlighted by an asterisk.

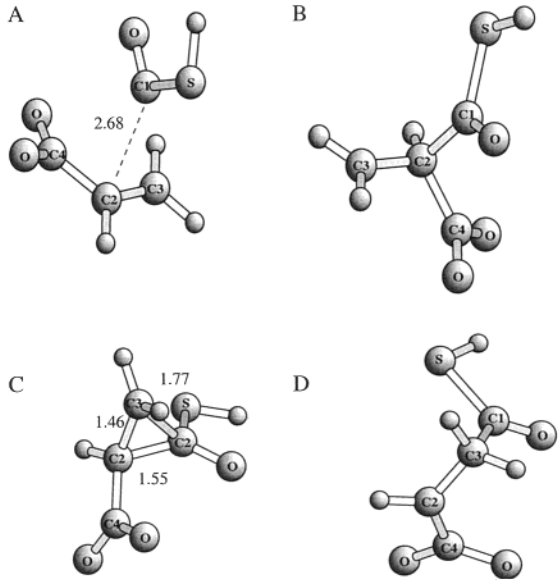

Figure 5. Stationary points of the rearrangement reaction. (A) Highly unstable intermediate of the fragmentation−recombination mechanism. (B) (2*R*)-*MMCoA*. (C) Transition state of the addition−elimination mechanism. (D) *SuccCoA*. Selected distances are shown in Å.

Influence of Potential Hydrogen Bond Donors. The optimized geometries for educt and product display the same hydrogen bonding pattern as is found in the X-ray structure, and also the arrangement of hydrogen bonds at the saddle point

(58) Frisch, M. J.; Trucks, G. W.; Schlegel, H. B.; Scuseria, G. E.; Robb, M. A.; Cheeseman, J. R.; Zakrzewski, V. G.; Montgomery, J. J. A.; S., E.; Burant, J. C.; Dapprich, S.; Millam, J. M.; Daniels, A. D.; Kudin, K. N.; Strain, M. C.; Farkas, O.; Tomasi, J.; Barone, V.; Cossi, M.; Cammi, R.; Mennucci, B.; Pomelli, C.; Adamo, C.; Clifford, S.; Ochterski, J.; Petersson, G. A.; Ayala, P. Y.; Cui, Q.; Morokuma, K.; Malick, D. K.; Rabuck, A. D.; Raghavachari, K.; Foresman, J. B.; Cioslowski, J.; Ortiz, J. V.; Stefanov, B. B.; Liu, G.; Liashenko, A.; Piskorz, P.; Komaromi, I.; Gomperts, R.; Martin, R. L.; Fox, D. J.; Keith, T.; Al-Laham, M. A.; Peng, C. Y.; Nanayakkara, A.; Gonzales, C.; Challacombe, M.; Gill, P. M. W.; Johnson, B.; Chen, W.; Wong, M. W.; Andres, J. L.; Gonzales, C.; Head-Gordon, M.; Replogle, E. S.; Pople, J. A. *Gaussian 98*, revision A.7; Gaussian, Inc.: Pittsburgh, PA, 1998.
(59) MacKerell, A. D.; Bashford, D.; Bellott, M.; Dunbrack, R. L.; Evanseck, J. D.; Field, M. J.; Fischer, S.; Gao, J.; Guo, H.; Ha, S.; Joseph-McCarthy, D.; Kuchnir, L.; Kuczera, K.; Lau, F. T. K.; Mattos, C.; Michnick, S.; Ngo, T.; Nguyen, D. T.; Prodhom, B.; W. E. R., III; Roux, B.; Schlenkrich, M.; Smith, J. C.; Stote, R.; Straub, J.; Watanabe, M.; Wiorkiewicz-Kuczera, J.; Yin, D.; Karplus, M. *J. Phys Chem. B* **1998**, *102*, 3586−3616.
(60) Brooks, C. L., III; Karplus, M. *J. Mol. Biol.* **1988**, *208*, 159−181.
(61) Levy, R. M.; Karplus, M.; McCammon, J. A. *Chem. Phys. Lett.* **1979**, *65*, 4.
(62) Brooks, C. L., III; Karplus, M. *J. Chem. Phys.* **1983**, *79*, 6312−6325.
(63) Brooks, C. L., III; Bruenger, A.; Karplus, M. *Biopolymers* **1985**, *24*, 843.

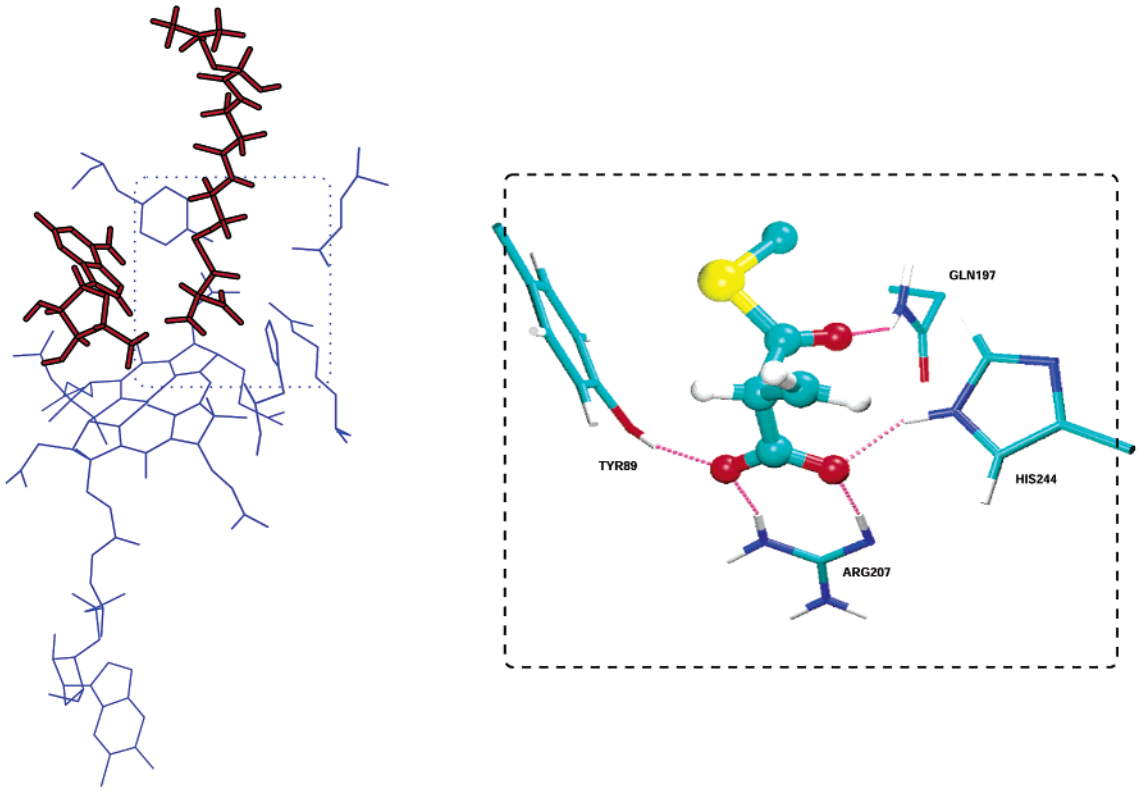

Figure 6. Structural arrangement of B_{12} cofactor and substrate. The boxed area is drawn enlarged (right) and shows the detailed geometry of the hydrogen bond donors.

geometry remains unchanged. ARG207 and TYR89 hydrogen bond to the carboxy group of the substrate. Also, GLN197 and HIS244 form hydrogen bonds with the acyl oxygen. A potential lowering of the rearrangement barrier by partial proton transfer from HIS244 has been a matter of debate in various experimental and theoretical studies.[41,64,65] Ab initio calculations suggest that protonation of the acyl oxygen considerably lowers the barrier and partial proton donation should result in a significant decrease. For an exact evaluation of the influence of partial proton transfer, the QM system was expanded. To produce more accurate geometries involving hydrogen bonds, a larger basis set (6-31+G(d,p)) was employed for the QM part of the hybrid QM/MM potential. The QM region comprised the original part of the substrate, the imizadole part of HIS244, and the formamide part of GLN197. The latter was chosen to be treated as QM atoms as this residue is located close to the acyl oxygen of the substrate in the X-ray structure and because of its action as a hydrogen bond donor, as was found in the earlier minimizations. For all subsequent QM/MM minimizations, the following trend was observed: The HIS244 moiety was displaced from the "ideal" hydrogen bond donor arrangement found earlier, where it points directly toward the acyl oxygen of the substrate, to a position approximately bisecting the angle to the carboxy and the carbonyl oxygen (angle N−H−O(4) ca. 140° and N−H−O(1) ca. 120°), but remaining close to the two acceptors (Figure 6). This trend was also confirmed by MD simulations (see below). The amide of GLN197 remained stable in a hydrogen bond donor position toward the acyl oxygen. From these geometries, a direct proton donation to the acyl oxygen is difficult to realize and is probably not the main catalytic source for this reaction, as was also found by experimental studies. Detailed energetics of the considered system can be found in Table 1. Again, the transition state shows a single imaginary frequency of wavenumber $\nu = 227$ cm^{-1}; the total vibrational energies, however, sum up to a disfavorable +0.71 kcal/mol for the transition state.

Table 1. Energies for the Addition−Elimination Pathway[a]

system	rel. energy [kcal/mol]	rel. energy + ZPE [kcal/mol]
small QM zone:		
MMCoA	0.0	
TS	+11.94	+11.73
SuccCoA	−2.45	−0.52
large QM zone:		
MMCoA	0.0	0.00
TS	+10.99	+11.70
SuccCoA	−5.08	−2.39

[a] Energies and zero-point corrected energies are shown for the original system and the system with an extended QM region.

To elucidate further the factors influencing the barrier height, several "in-silico" mutations have been performed. The imidazole ring of HIS244 was replaced by a hydrogen; GLN197 was modified to ALA197 and TYR89 to PHE89. All of the following calculations have been performed as full QM/MM minimizations for educt and product with the above-mentioned protocols; however, because of computational cost, the geometry of the cyclopropyloxy fragment of the saddle point was constrained to the position calculated before. As the geometries of educt and product did not significantly change during these calculations, the same can be assumed for the saddle point geometry. However, the calculated energies should be considered as

(64) Maiti, N.; Widjaja, L.; Banerjee, R. *J. Biol. Chem.* **1999**, *274*, 32733−32737.
(65) Thomä, N. H.; Evans, P. R.; Leadley, P. F. *Biochemistry* **2000**, *39*, 9213−9221.

Table 2. Effect of Mutations on the Energy[a]

mutation	rel. energy [kcal/mol]	rel. energy vs unmutated system [kcal/mol]
His244Ala + *MMCoA*	0.0	
His244Ala + *MMCoA* → His244Ala + *SuccCoA*	+12.87	+1.88
His244Ala + *SuccCoA*	−3.40	+1.68
Gln197Ala + *MMCoA*	0.0	
Gln197Ala + *MMCoA* → Gln197 + *SuccCoA*	+12.45	+ 1.46
Gln197Ala + *SuccCoA*	−4.54	+ 0.54
Tyr89 + *MMCoA*	0.0	
Tyr89 + *MMCoA* → Tyr89 + *MMCoA*	+11.44	
Tyr89 + *SuccCoA*	−2.21	
Tyr89Phe + *MMCoA*	0.0	
Tyr89Phe + *MMCoA* → Tyr89Phe + *MMCoA*	+12.44	+1.0
Tyr89Phe + *SuccCoA*	−2.24	−0.03

[a] The relative energies are shown in the middle column; the differences to the unperturbed system, where available, are shown in the right column.

perturbations to the originally optimized structures and depict the energetic consequences of a varying nonbonding environment rather than as supplying exact geometries. For this reason, the results listed in Table 2 explicitly display the energetic consequences of a mutation as compared to the original system.

The following conclusions can be drawn from Table 2: HIS244 lowers the barrier by 1.88 kcal/mol. This is a slightly lower catalytic gain as compared to the measured rate reduction by a factor of 10^2-10^3,[64,65] but it is in the range of the numerical and methodological inaccuracy of density functional methods.[66] The influence of hydrogen bond donation by GLN197 is in the same range, stabilizing the activation energy by 1.46 kcal/mol. The effect of TYR was found to be −1.0 kcal/mol, which is also slightly lower than what might be expected from experimental isotope labeling studies.[67] Altogether, these residues might well account for the reduction of the barrier from a value of 15.36 to 10.6 kcal/mol (we refer here to the high-quality calculations of Smith et al.[41] for systems in vacuo), but with stabilization resulting from several hydrogen bond donors rather than a single proton donation. The electrostatic and van der Waals interactions of the considered residues were additionally analyzed by calculating atomic charges of the QM atoms. The algorithm fits charges on atoms such that the electrostatic field is optimally reproduced (see, e.g., ref 57). The results for selected atoms can be found in Table 3. From these data, it can be concluded that HIS244 stabilizes educt, transition state, and product likewise as the charge polarization is reduced as compared to the mutant. GLN197 shows a comparable stabilization for the transition state and SuccCoA. The induced charges are localized on the acyl group and the neighboring atoms, whereas the carboxy group charges remain mainly unchanged by these variants. For the alteration TYR89PHE, it is mainly the hydrogen-bond accepting oxygen of the carboxy group which shows an increased charge upon mutation.

To examine further the origin of the catalytic power of this reaction, the *MMCoA* fragment was cut out of the enzyme, and an ab initio minimization in vacuo was performed. Besides elongation of the bond from the acyl carbon to the sulfur atom,

(66) Durant, J. L. *Chem. Phys. Lett.* **1996**, *256*, 595−602.
(67) Thomä, N. H.; Meier, T. W.; Evans, P. R.; Leadley, P. F. *Biochemistry* **1998**, *37*, 14386−14393.

Table 3. Selected Atomic Charges of the Different Systems Examined[a]

	atom name	wild-type	HIS244ALA	GLN197ALA
MMCoA:	O1	−0.44	−0.51	−0.43
	C1	+0.25	+0.42	+0.31
	C2	+0.38	+0.25	+0.45
	C3	−0.62	−0.53	−0.67
TS:	O1	−0.48	−0.54	−0.42
	C1	0.30	+0.44	+0.53
	C2	0.13	+0.12	+0.04
	C3	−0.49	−0.44	−0.49
SuccCoA:	O1	−0.37	−0.52	−0.48
	C1	0.35	+0.58	+0.40
	C2	−0.05	0.02	+0.14
	C3	−0.29	−0.32	−0.55

[a] In general, the systems without catalytically active residues show increased charges as compared to the wild-type system. For the mutant GLN197ALA, this refers predominantly to the transition state and the product.

which can be expected, no significant change of the "hard" degrees of freedom (bond lengths, angles) was found. All other bonds changed by less than 0.15 Å, and the angles varied up to ±3°. However, in the vacuum structure, the thioester group rotated along the axis C1−C2 such that the bonds C1−O1 and C2−C3 are in a plane. Thus, it may be assumed that no essential labilization of the substrate by preferential binding of the transition state analogue occurs in *MMCoA* mutase.

Stereochemistry of the Reaction *SuccCoA* → *MMCoA*. Apart from the stabilizing effect of TYR89, this residue is believed to be essential for controlling the stereoselectivity of the reverse reaction. From isotope labeling experiments, it is known that stereoselectivity toward the *R*-isomer of *MMCoA* is strict, whereas it is incomplete toward discrimination of the two hydrogens of the prochiral center C3. To examine further these findings, three molecular dynamics simulations were performed: a simulation of the wild-type, of the mutant TYR89PHE, and of the mutant TYR89GLY. All simulations were performed for a length of 1000 ps with a stochastic boundary protocol as described in Computational Methods. The trajectories were analyzed from 150 ps, when the system was assumed to have equilibrated, as the trajectories showed stable total energies and constant rms values. Two aspects were analyzed in detail: the occurrence of a preferential abstraction of one of the hydrogens, and the steric requirements of the radical intermediate. For the former, the distance from both the enantiotopic hydrogens to the C5′ of deoxyadenosyl was measured as well as the torsion angle C2−C3, which was found to be the significant motion of translocation of the hydrogens. For the wild-type simulation, it was found that, although the simulation was started with one of the hydrogens in close proximity to C5′, the other hydrogen is positioned by a rotation around the torsion axis C2−C3 in the sterically preferred position for abstraction. This effect is much less distinct in the mutant TYR89PHE simulation, where the average distance of the two enantiotopic atoms to C5′ is approximately the same. For the TYR89GLY mutation, the preferential arrangement of the two hydrogens is inverted as compared to the wild-type. Figure 7b depicts the torsion angles of the mutants, which can be seen to differ significantly from that of the wild-type.

The subsequent step in the catalytic cycle involves formation of *MMCoA*. From the succinyl-CoA intermediate, formation of both enantiomers is, in principle, possible; thus, TYR89 could

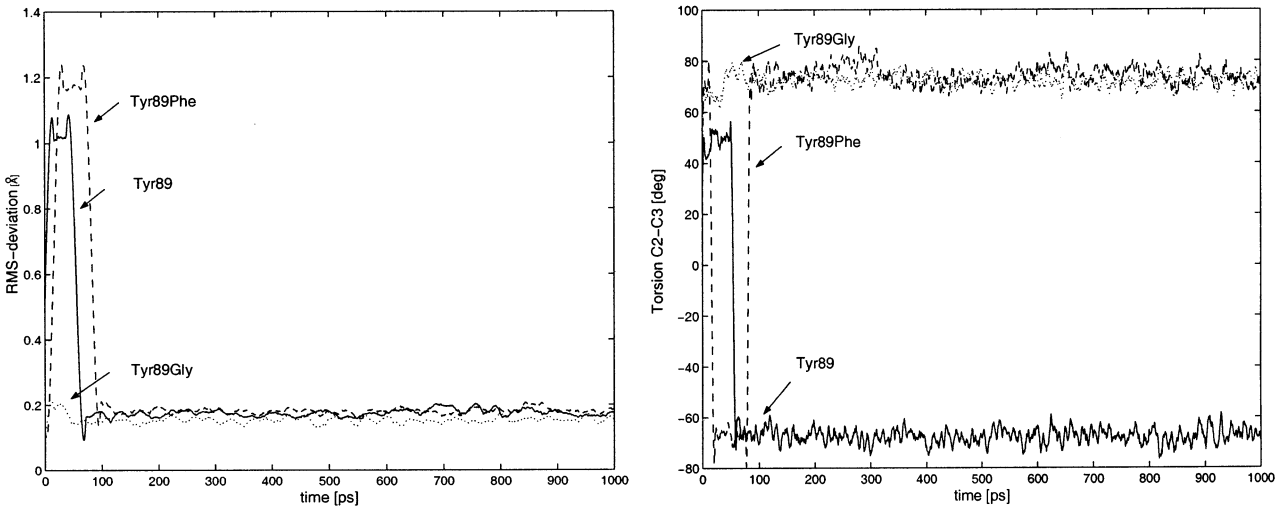

Figure 7. Left: The rms values of the succinate part of the substrate are drawn for the three variants. After being heated, they remain stable with approximately the same magnitude. Right: The torsion angles show distinct differences between TYR89 ($\sim -70°$) and the two mutants ($\sim 70°$). Rotations along the torsion axis are possible but seem to be rare events.

restrict the available space for succinyl-CoA such that the reaction is guided toward the (2*R*)-isomer of *MMCoA*, or limit the flexibility of the bound substrate, thus "cramping" it into the correct position. A possible enhancement of flexibility of the bound substrate by the mutants was examined by calculation of the rms values of the succinate part of the substrate. The rms values have been calculated with respect to the averaged structure and are shown in Figure 7a. No significant changes in the flexibility of the bound substrate can be recognized, and it must be thus concluded that the hydrogen bond of TYR89 to the substrate is not essential for restraining the substrate in a position which induces selective formation of the (2*R*)-isomer of *MMCoA*. Rather, it is the presence of a bulky side chain that prohibits formation of one of the stereoisomers. This finding is consistent with the observation that the average position of the side chain of TYR89PHE is the same as that of the side chain of TYR89, and with the experimental result that the mutation TYR89PHE only slightly reduces catalytic activity.[67]

Conclusions

Two mechanisms for the 1,2-rearrangement reaction of *MMCoA* mutase have been studied by means of QM/MM techniques. On the basis of energetic arguments, the mechanism involving a cyclopropyloxy radical, which is proposed as a saddle point, is the dominant one. The calculated barrier for this isomerization step is found to be 10.78 kcal/mol, which is a considerable decrease as compared to the vacuum value. Several factors contribute to this lowering, but in this study no predominant effect from partial hydrogen transfer can be found, which has also been confirmed in experimental studies. The hydrogen bonding pattern indicates hydrogen bonding from HIS244 and TYR89 to the carboxy oxygens of *MMCoA*, and apparently these interactions contribute 1−2 kcal/mol each to a reduction of the barrier. An amide hydrogen of Gln197 interacts with the carbonyl oxygen and thus partially activates the isomerization by lowering the transition state. The structural arrangements found were independently confirmed by MD simulations.

The stereoselective directing effect of TYR89 was examined by MD studies of the wild-type and two mutants. The loss of a hydrogen bond or even of the whole phenolic side chain does not result in increased flexibility of the bound substrate as was evidenced by rms values of the bound substrate and by the largely coincident position of the side chains of TYR89 and TYR89PHE. Therefore, the hydroxyl group seems not to be essential for directing stereochemistry. The preferential abstraction of one of the hydrogen atoms of succinate, however, is influenced by the choice of mutations.

Acknowledgment. M.J.L. thanks W. G. Richards for his hospitality in Oxford, where most of the work was carried out. This work was supported by a grant of the Austrian Science Fund (grant number P13845-TPH).

JA028906N